

Fully Automated R-peak Detection Algorithm (FLORA) for Fetal Magnetoencephalographic Data

Katrin Sippel^{a,b,*}, Julia Moser^b, Franziska Schleger^b, Hubert Preissl^{b,c},
Wolfgang Rosenstiel^a, Martin Spüler^a

^a*Eberhard-Karls-University of Tuebingen, Wilhelm-Schickard- Institute for Computer
Science - Computer Engineering Department, 72076 Tuebingen*

^b*Institute for Diabetes Research and Metabolic Diseases (IDM) of the Helmholtz Center
Munich at the University of Tuebingen, fMEG Center; German Centre for Diabetes
Research (DZD), 72076 Tuebingen*

^c*Eberhard-Karls-University of Tuebingen, Interfaculty Centre for Pharmacogenomics and
Pharma Research, Department of Pharmacy and Biochemistry, 72076 Tuebingen*

Abstract

Background and Objective: Fetal magnetoencephalography (fMEG) is a method for recording fetal brain signals, fetal and maternal heart activity simultaneously. The identification of the R-peaks of the heartbeats forms the basis for later heart rate (HR) and heart rate variability (HRV) analysis. The current procedure for the evaluation of fetal magnetocardiograms (fMCG) is either semi-automated evaluation using template matching (SATM) or Hilbert transformation algorithm (HTA). However, none of the methods available at present works reliable for all datasets.

Methods: Our aim was to develop a unitary, responsive and fully automated R-peak detection algorithm (FLORA) that combines and enhances both of the methods used up to now.

Results: The evaluation of all methods on 55 datasets verifies that FLORA outperforms both of these methods as well as a combination of the two, which applies in particular to data of fetuses at earlier gestational age.

Conclusion: The combined analysis shows that FLORA is capable of providing

*Corresponding author

Email address: katrin.sippel@uni-tuebingen.de (Katrin Sippel)

good, stable and reproducible results without manual intervention.

Keywords: magnetocardiography

1. Introduction

Fetal magnetoencephalography (fMEG) facilitates the investigation of fetal brain and autonomic nervous system development [1, 2]. Like magnetoencephalography in children and adults [3], fMEG is a noninvasive method. It is primarily used to measure auditory or visually event related brain responses of the fetus [4, 5, 6, 7, 8, 9] as well as spontaneous brain activity [10, 11]. With its good spatio-temporal resolution, it also allows to monitor maternal (mMCG) and fetal magnetocardiograms (fMCG) simultaneously to the recording of fetal brain activity (see Fig. 2). This enables us to additionally evaluate maternal and fetal heart rate (HR), different parameters of heart rate variability (HRV) [12] and fetal behavioural states [13, 14], starting at 20 weeks of gestational age. Identification of the R-peaks [15] of the heart activity (see Fig. 3) forms the basis of HR and HRV analysis. The challenge of a good R-peak detection algorithm is to find as many R-peaks as possible and reduce the number of false negative (FN) peaks without detecting false positive (FP) peaks such as movement artifacts. Both a low number of FN and a low number of FP peaks should result in a number of peaks per minute in the range of the natural heart rate, and small and well-distributed distances between consecutive R-peaks (RR-interval). While too many FN peaks lead to a too low heart rate and huge RR-intervals, too many FP peaks cause a too high heart rate estimation, too small RR-intervals and a lower signal-to-noise ratio (SNR).

A combination of semi automated evaluation by experts using template matching (SATM) and the automated Hilbert transformation approach (HTA) [16] is the standard procedure for both maternal and fetal R-peak detection. Both of these commonly used methods function for most maternal heart evaluations since the representation of the maternal heart signal is quite strong and virtually stationary. In fetal HR, however, the evaluation is somewhat more difficult.

Since the mMCG signal is between 10 and 100 times stronger than the fMCG signal, the maternal heart signal must first be removed from the data before fetal heart evaluation can be carried out. In addition, the strength of the detected heart activity is highly dependent on the quality of the recording, gestational age and position of the fetus. It is even more difficult to detect the fMCG signal when it is superimposed by muscle artifacts or if the fetus moves during the recording. For both HR and HRV analysis, the maternal/fetal heart activity must be detected as comprehensively and as precisely as possible. For critical and noisy dataset, the previously used methods tend to be either complete or precise but not both.

SATM requires the manual selection of one heartbeat as a template (see section 2.2.1). This template is then used to locate and mark all similar heartbeats in the dataset. One dataset contains the information of 156 sensors over the whole recording time. Since template matching works for the data of each sensor individually, it achieves high accuracy results for stable recordings. However, if the mother or the fetus moves during the measurement, this method is at a disadvantage since the fetal heart signal then no longer fits the template. This could lead to a long gap in R-peak detection of up to several minutes per dataset. Nevertheless, semi-automated evaluation is generally much more flexible than fully automated evaluation. Due to manual interventions it is possible to meet the individual demands of a specific dataset (e.g. the deactivation of very noisy sensors), making it difficult for fully automated algorithms to achieve comparable results. By contrast, the HTA generates a single signal for all sensors which is an advantage for non-stationary measurements (see section 2.2.2). However, if the overall noise level is too high, movements of the fetus could cover the real R-peak or could be misinterpreted as an additional peak, leading to a loss of accuracy and quality.

A continuous and precise R-peak identification must therefore be performed by a combination of both methods to ensure that the majority of datasets are validly evaluated. Since this is a complex and very time-consuming procedure, we aimed to develop an fully automated R-peak detection algorithm (FLORA)

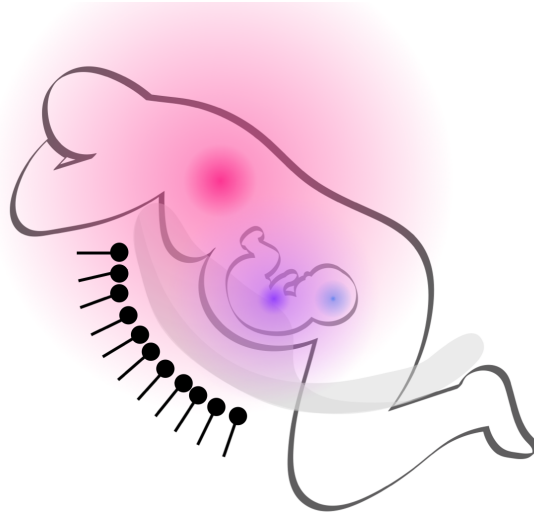


Figure 1: Sketch of the fMEG device

which combines the advantages of both previously used methods, automatically
60 detects sensors with high physiological or non-physiological noise and is adaptive
to the real heart rate in each dataset. It is also aimed to eliminate erroneously
detected heart beats and fill in missing peaks automatically to evaluate fMEG
data rapidly and at the same time as effectively as manual guided evaluation.
This paper describes how FLORA functions and compares its performance not
65 only to the two established methods, but also to a combination of the two.

2. Methods

2.1. Fully automated R-peak detection algorithm (FLORA)

FLORA can be divided into four main steps: First, a noise analysis is per-
formed. Second, the heart frequency of the raw dataset is analyzed to identify
70 the individual characteristics of each recording. Third, R-peaks are detected
by combining three different approaches. Fourth, contingently existing gaps are
filled step by step. This procedure is the same for both maternal and fetal
R-peak detection. Each of these steps will be explained in more detail in the
following (the workflow of FLORA is depicted in Figure 2).

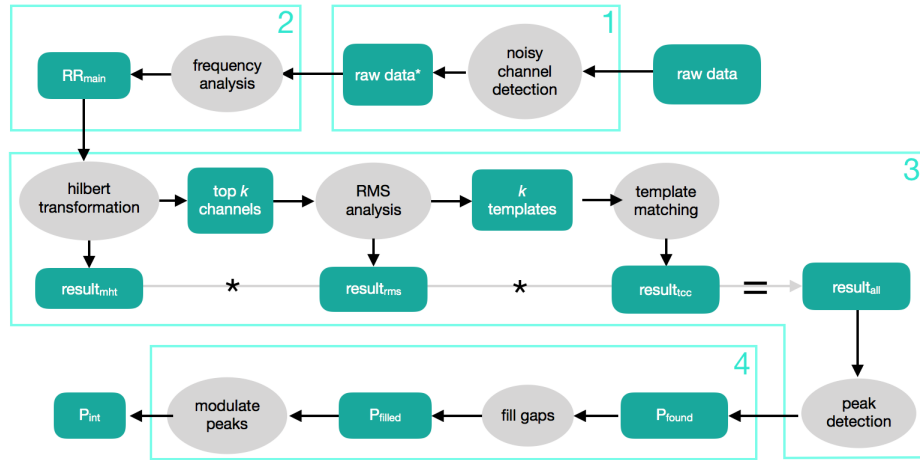


Figure 2: Sketch of the FLORA algorithmic procedure

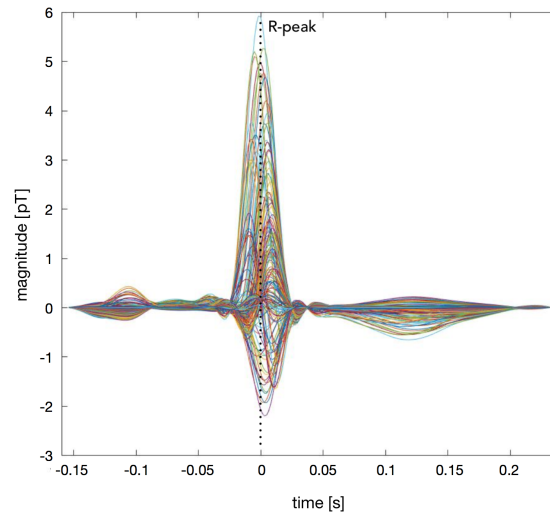


Figure 3: Shape of averaged fetal heart beats over one dataset. Time point 0 refers to the detected R-peaks (the moment of highest magnetic activity during one heartbeat).

75 *2.1.1. Noisy sensor detection*

It is possible that some of the 156 single sensors show some unspecific noise caused by defect sensors, a tattoo or the retainer of the pregnant woman. Such sensors impede the evaluation of the dataset and should be removed before

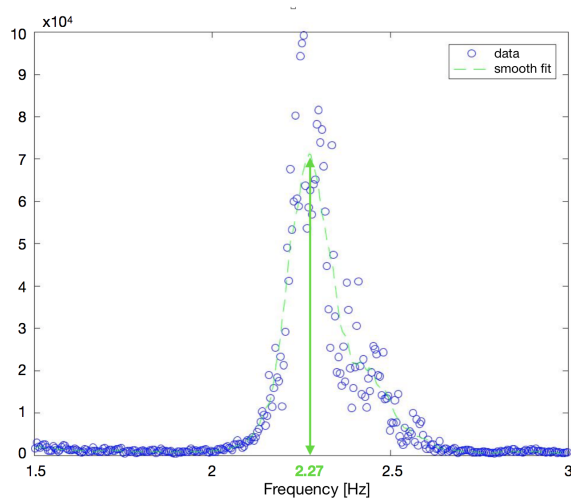


Figure 4: Frequency between 1.5 and 3 Hz of one dataset, after removal of the maternal heart interference. In this case $f_{nat} = 2.27$ which matches $RR_{main} = 0.44$ and a mean HR of about 136 bpm.

data processing. Since these sensors show high signal variance and/or very low
 80 correlation to the signal of their neighbor sensors they can be easily identified
 and set to zero.

2.1.2. Frequency analysis

The aim of the frequency analysis is to identify the individual heart rate
 characteristic of each dataset. Therefore, a fast Fourier spectral analysis is
 85 performed of the whole dataset. The result of the spectral analysis is smoothed
 by a moving average window of 20 datapoints. The frequency at the maximum
 of this curve represents the main natural frequency of the HR f_{nat} (see Fig. 4).
 The window for maternal frequency analysis is 0.8-2.2 Hz (corresponds to a HR
 of 48 - 132 bpm) and 1.5-3 Hz (corresponding to a HR of 90 - 180 bpm) for
 90 fetal. The resulting main RR-interval $RR_{main} = 1/f_{nat}$ is used as parameters
 for further analysis (see Fig. 2).

2.1.3. Peak detection

Hilbert transformation. The magnitude of the Hilbert transformation is calculated for all sensors and all sampling points (t), resulting in a vector ($result_{mht}$)
95 with dimension $1 \times t$, rendering this kind of search resistant to fetal movements. R-peaks are identified by a top-down peak search that commences with the highest maximum point in the transformed dataset and continues with the next maximum with a minimum distance d_{min} to the recent one. This minimum distance is defined by the result of the frequency analysis: $d_{min} = RR_{main} * 0.7$.
100 Factor 0.7 is chosen since it is assumed that the HR does not deviate more than 30% from the main RR-interval RR_{main} . Subsequently, the average over the whole dataset at the time points of all detected heartbeats (P_h) is calculated and k sensors with the highest absolute R-peak value are selected ($k = 20$ for maternal, $k = 5$ for fetal MCG).

105 *RMS analysis and template generation.* Having taken the signal of the selected k sensors, a matrix with dimension $k \times t$, the root mean square (RMS) over the k sensors at each sampling point t is calculated resulting in a vector ($result_{rms}$) with dimension $1 \times t$. Peak detection is performed with the same parameters as in the previous step. The result is averaged over all peak times (P_v) to generate
110 one template for each of the k sensors. Each template has the length of the average RR-interval, with 40% of the time before and 60% after the R-peak. This procedure is adopted to ensure that the characteristics of the P, Q, S and T wave are enclosed.

Template matching. After generating the template by the RMS analysis, the
115 cross-correlation between the template and the signal is calculated for each of the k sensors individually. These k cross correlations are summed up to a general template cross-correlations vector ($result_{tcc}$) with dimension $1 \times t$.

Combination of results. To combine the results of the previous three analysis steps, the product of their resulting curves is calculated:

120 $result_{all} = result_{mht} * result_{rms} * result_{tcc}$

A final peak search is performed on $result_{all}$ using the minimum peak distance d_{min} and a minimum peak height of 0, since the baseline of $result_{all}$ is negative. The thereby detected R-peaks (P_{found}) are used for further analysis.

Interpolation of missing peaks. By dividing all resulting RR-intervals by RR_{main} ,
125 gaps in the R-peak detection can be easily identified. The number of missing
beats is subsequently calculated by dividing the size of the gap by the mean of
the HR before and after the gap. The gaps are initially filled by dividing the
length of the gap by the number of missing beats (m) + 1 and thereby creat-
ing m artificial peak time points. Since such an artificial filling would have a
130 profound effect on measures like the HRV, the algorithm searches for additional
peaks of $result_{all}$ in the time window of ± 20 ms around the artificial time point.
These artificial time points are then replaced by the the highest peak in this
time window. The final number of detected R-peaks in FLORA (NP_{FLORA}) is
the sum of detected peaks (P_{found}) and interpolated peaks (P_{int}).

135 2.2. Comparison to standard methods

To evaluate the performance of FLORA, the algorithm was compared to
both previously used methods SATM and HTA as well as to the combination
of both methods.

2.2.1. Semi Automated Template Matching (SATM)

140 This section describes template matching as implemented in the Data Edi-
tor Software, which is the standard software provided by the fMEG hardware
manufacturer (VSM MedTech Ltd.). Prior to R-peak detection, the dataset
is detrended and filtered with a bandpass filter from 1-35 Hz . The user is
requested to mark a regular heart beat manually which is subsequently used
145 as a template for template-matching R-peak detection. The resulting R-peaks
(P_{SATM}) are exported to a marker-file.

2.2.2. Hilbert Transformation Approach (HTA)

This approach by Wilson et al. [16] uses Hilbert transformation. Prior to
R-peak detection, the dataset is filtered with a Butterworth bandpass filter from

150 1-60 Hz . A Fast Fourier Transformation of each sensor is carried out to calculate
the sum of the power at each frequency afterwards. The Hilbert transformation
is calculated on the 10 sensors with the highest power sum. The algorithm
works with an upper (210 bpm) and lower (100 bpm) limit for the fetal heart
rate (40 - 110 bpm for maternal heart rate). Threshold values are used to locate
155 the peaks in Hilbert-transformed data which indicate the heartbeats (P_{HTA}).

2.2.3. Combination of SATM and HTA (COMB)

For standard analysis of our fMEG studies, always both methods are applied
after each other to get the best heart beat detection for the existing datasets.
The result in which more R-peaks are detected is usually chosen for further
160 evaluation. Using these standard methods, an additional visual check is always
necessary to ensure that a higher number of peaks is not caused by arbitrarily
added peaks. With regard to the 55 selected datasets in this evaluation, the
evaluation by an expert found SATM to be more precise for 21 datasets and
HTA better for the other 34 datasets. This combination is denoted as COMB
165 below.

2.3. Evaluation

Data was recorded by a 156 sensor SARA (SQUID Array for Reproduc-
tive Assessment, VSM MedTech Ltd., Port Coquitlam, Canada) system at the
University of Tuebingen with a sampling rate of 610 or 1220 Hz . In total, 55
170 datasets of singleton pregnant women were evaluated. The gestational age of
the fetuses ranged from 26 to 39 weeks (mean 30.89 ± 3.31). The length of the
recordings varied between 6 and 27 minutes (mean 12.96 ± 5.73) and included
both spontaneous data and different stimulation paradigms. Prior to process-
ing, the raw dataset is filtered with a Butterworth band pass filter from 1 to
175 35 Hz . Four metrics were used to evaluate the detection methods which are
explained in more detail in the following sections.

2.3.1. Number of detected peaks per minute (NP)

The number of R-peaks found in the dataset is the first indicator for the quality of the algorithm. Although in general, less peaks are found in critical datasets, particularly when using the HTA, it could also be that fetal movements are misinterpreted as R-peak which in turn would lead to higher NP and lower SNR (see 2.4 and 2.4.1). Nevertheless, the NP for fetal analysis should produce results in the normal range of fetal heart rate (120 - 160 bpm).

185

2.3.2. Difference between RR measures (RR-DIFF)

A mean HR of healthy fetuses of between 120 and 160 bpm results in a normal RR-interval of between 0.375 and 0.5 seconds. The histogram of a HR recording should therefore resemble a Gaussian distribution of the RR-interval with a peak within that range. The more gaps there are in the analysis, the higher the mean RR-interval will be, and the more additional noise peaks the algorithm finds, the lower the mean RR-interval will be. Due to the fact that the mean RR-distance is dependent on the behavioral state of the fetus and that it could also change over gestational age, the main natural RR-interval RR_{main} is calculated by extracting the main frequency f_{nat} using a frequency analysis of the data as described in Figure 4. The more continuously the R-peak detection works, the lower the difference RR-DIFF between RR_{main} and the mean RR-interval RR_{est} of the estimated HR will be. This parameter compares how close NP and RR are to the average heart rate/heart frequency of each dataset.

195

$$RR_{main} = \frac{1}{f_{nat}} \quad (1)$$

200

$$RR_{diff} = |RR_{main} - RR_{est}| \quad (2)$$

2.4. Percentage of normal to normal intervals (PNN)

The percentage of normal to normal (PNN) is the amount of normal RR-intervals. 'Normal' in this case is defined as all RR_{est} values between $RR_{main}/2$ and $2 * RR_{main}$. Since the normal-to-normal and other parameters of the heart

205 rate are generally used for HRV analysis, a high PNN is important for a valid HRV result. While in the RR-DIFF value many smaller gaps do not weigh as heavily as one very big gap, the opposite applies with regard to the PNN.

2.4.1. Signal to noise ratio (SNR)

210 Although the above-mentioned measurements give us an indication about the reliability of the algorithms, they cannot guarantee that the R-peaks added by FLORA correspond to real R-peaks and are not just arbitrary added points. Therefore, the SNR of the averaged RR-peaks (see Fig. 3) of the raw data is calculated, where amp_{peak} describes the height of the amplitude at the R-
215 peak which is then divided by the median of the amplitude over the whole average sample. Precisely located R-peaks would result in a high SNR, whereas arbitrary added R-peaks would result in a lower amplitude at the time of the R-peaks amp_{peak} , and in more noise over the whole averaged sample (higher $median(amp)$) and therefore in a lower SNR.

$$SNR = \frac{amp_{peak}}{median(amp)} \quad (3)$$

2.4.2. Statistics

220 SATM, HTA and COMB were compared against FLORA in all four metrics by using a Wilcoxon Signed Rank Test. To decide whether a result is significant, the significance levels were adjusted by Bonferroni correction to $p = frac{0.053}$. Due to extreme outliers in the results, it was decided to report [median \pm
225 standard deviation] instead of the mean.

3. Results

FLORA algorithm was analyzed for maternal and fetal R-peak detection. Maternal R-peak detection is easily performed and works very well for all three algorithms. Hence, there were no obvious differences and the following results
230 relate to fetal R-peak detection only.

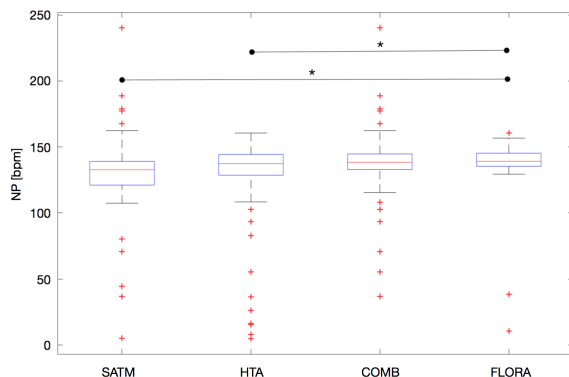


Figure 5: Number of R-peaks, identified per minute. *denotes significant differences in the Wilcoxon signed rank test ($p < 0.05$), Bonferroni corrected for multiple comparison.

3.0.1. Number of detected peaks per minute (NP)

A comparison of the number of heart beats (NP) per minute as obtained with the four different methods showed a significant difference between SATM [132.67 \pm 36.86] and FLORA [139.17 \pm 23.15] as well as between HTA [137.40 \pm 41.05] and FLORA. No significant difference is observed between COMB [138.35 \pm 29.24] and FLORA (see Fig. 5).

3.0.2. Difference between RR measures (RR-DIFF)

The difference between RR_{main} and the mean RR-interval RR_{est} of the estimated HR also showed a significant difference between SATM [0.01 \pm 1.57] and FLORA [0.001 \pm 0.72] as well as HTA [0.005 \pm 1.96] and FLORA. Again, no significant difference is found between COMB [0.004 \pm 0.20] and FLORA (see Fig. 6).

3.1. Percentage of normal to normal intervals (PNN)

The PNN showed significant differences between FLORA [100 \pm 5.81] and all other methods, SATM [98.48 \pm 19.26], HTA [99.97 \pm 23.16] and COMB [99.85 \pm 14.57] (see Fig. 7).

In Figure 8 the PNN with regard to gestation age (GA) is displayed for FLORA, SATM and HTA. The figure shows that especially for fetuses with lower GA

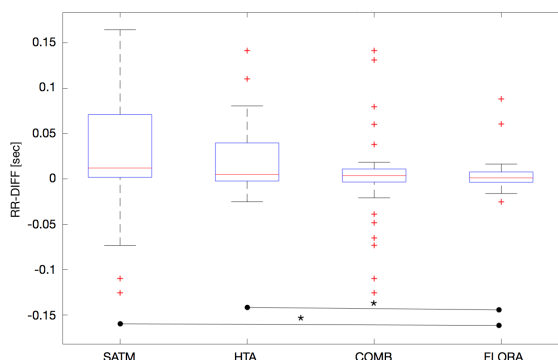


Figure 6: The difference between RR_{nat} and the averaged RR-interval RR_{est} as estimated by the different R-peak detection methods. *denotes significant differences in the Wilcoxon signed rank test ($p < 0.05$), Bonferroni corrected for multiple comparison.

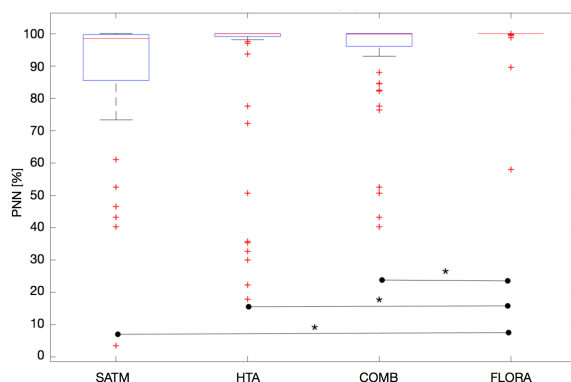


Figure 7: The percentage of normal RR-intervals. *denotes significant differences in the Wilcoxon signed rank test ($p < 0.05$), Bonferroni corrected for multiple comparison.

both, SATM and HTA result in lower PNN than FLORA. Figure 9 displays the
 250 PNN with reference to the measurement duration. FLORA in contrast to the
 other methods shows a high PNN also in short time measurements (see Fig. 9).

3.2. Signal to noise ratio (SNR)

The SNR of FLORA [20.38 ± 4.50] is significantly different to SNR of HTA
 [17.83 \pm 6.48]. No significant difference is shown between FLORA and SATM
 255 [20.03 \pm 6.62], or COMB [19.34 \pm 5.43] (see Fig. 10).

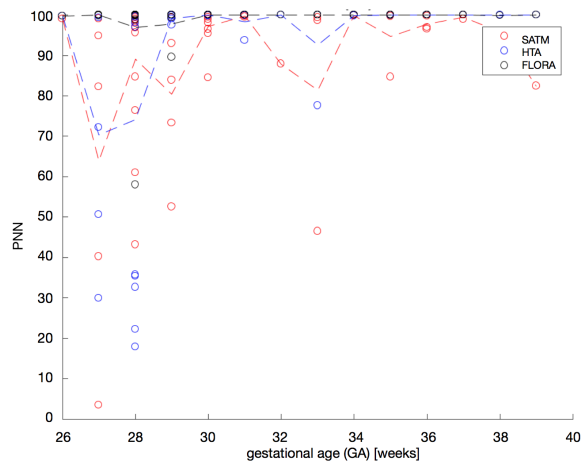


Figure 8: The relation of the gestational age (GA) of the fetus and the amount of normal RR-intervals in percent (PNN).

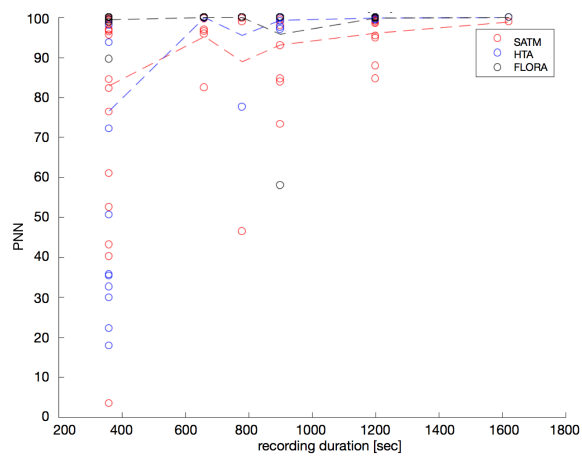


Figure 9: The relation of the measurement duration and the amount of normal RR-intervals in percent (PNN).

4. Discussion and Conclusion

Since FLORA was developed to perform fully automated R-peak detection, its performance was tested on 55 different real datasets and compared it with the currently established procedures. Four different evaluation metrics were used to compare performance between the different approaches. Our results show that

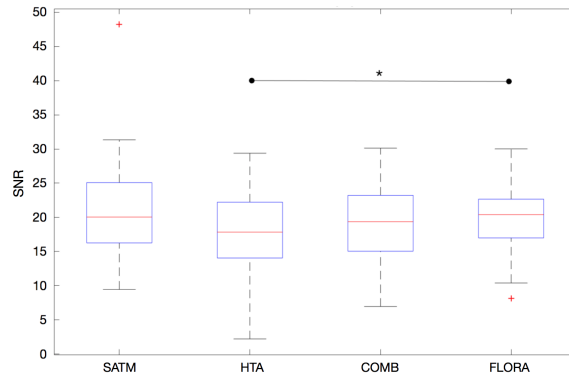


Figure 10: The SNR shows how clearly the R-peak contrasts from the rest of the averaged heart signal. *denotes significant differences in the Wilcoxon signed rank test ($p < 0.05$), Bonferroni corrected for multiple comparison.

FLORA not only performs just as well as the established methods SATM and HTA and their combination COMB but also that it has some advantages over these. FLORA is significantly more accurate in number of detected peaks per minute (NP) than SATM and HTA and the difference between RR measures (RR-DIFF) of FLORA is also considerably lower. Even if there is no significant difference in NP and RR-DIFF between FLORA and COMB, FLORA is convincing in percentage of normal to normal intervals (PNN) , where the results are significantly different from those of the standard methods SATM and HTA as well as to their combination COMB. Based on the results PNN it could be shown that FLORA works reliable over the whole GA range and is independent of the measurement duration. FLORA resulted in a significantly higher signal to noise ratio (SNR) than HTA, indicating that despite the higher NP the peaks derive from heartbeats that were actually detected and not from randomly added points. In sum, FLORA is user-independent which is very important for reproducibility. By removing noisy sensors, estimating the physiological heart rate of the subject, optimizing the peak search, filling gaps and modulating the interpolated peaks, FLORA generates high quality HR datasets that can be easily post-processed. Due to its automatization, FLORA can also be used for batch processing.

280 **Acknowledgment**

This work was partially supported by the Luminous project (EU-H2020-FETOPEN GA No.686764), the Helmholtz Alliance ICEMED-Imaging and Curing Environmental Metabolic Diseases and German Research Foundation (TR-SFB 654 Plasticity and Sleep) and a grant from German Research Foundation (DFG - DR 807/1-1).

References

- [1] H. Preissl, C. L. Lowery, H. Eswaran, Fetal magnetoencephalography: current progress and trends, *Experimental neurology* 190 (2004) 28–36.
- [2] H. Preissl, C. L. Lowery, H. Eswaran, Fetal magnetoencephalography: viewing the developing brain in utero, *International review of neurobiology* 68 (2005) 1–23.
- [3] R. Hari, S. Baillet, G. Barnes, R. Burgess, N. Forss, J. Gross, M. Hämläinen, O. Jensen, R. Kakigi, F. Mauguière, et al., Ifcn-endorsed practical guidelines for clinical magnetoencephalography (meg), *Clinical Neurophysiology*.
- [4] K. Linder, F. Schleger, I. Kiefer-Schmidt, L. Fritsche, S. Kümmel, M. Heni, M. Weiss, H.-U. Häring, H. Preissl, A. Fritsche, Gestational Diabetes Impairs Human Fetal Postprandial Brain Activity, *The Journal of Clinical Endocrinology & Metabolism* 100 (11) (2015) 4029–4036. doi:10.1210/jc.2015-2692.
- [5] F. Schleger, K. Landerl, J. Muenssinger, R. Draganova, M. Reinl, I. Kiefer-Schmidt, M. Weiss, A. Wacker-Gußmann, M. Huotilainen, H. Preissl, Magnetoencephalographic Signatures of Numerosity Discrimination in Fetuses and Neonates, *Developmental Neuropsychology* 39 (4) (2014) 316–329. doi:10.1080/87565641.2014.914212.

- [6] J. Muenssinger, T. Matuz, F. Schleger, R. Draganova, M. Weiss, I. D. Kiefer-Schmidt, A. Wacker-Gussmann, R. B. Govindan, C. L. Lowery, H. Eswaran, et al., Sensitivity to auditory spectral width in the fetus and infant—an fmeg study, *Frontiers in human neuroscience* 7 (2013) 917.
- 310 [7] R. Draganova, H. Eswaran, P. Murphy, C. Lowery, H. Preissl, Serial magnetoencephalographic study of fetal and newborn auditory discriminative evoked responses, *Early human development* 83 (3) (2007) 199–207.
- [8] L. Moraru, R. Sameni, U. Schneider, J. Haueisen, E. Schleußner, D. Hoyer, Validation of fetal auditory evoked cortical responses to enhance the assessment of early brain development using fetal meg measurements, *Physiological measurement* 32 (11) (2011) 1847.
- 315 [9] M. Chen, B. D. Van Veen, R. T. Wakai, Linear minimum mean-square error filtering for evoked responses: Application to fetal meg, *IEEE transactions on biomedical engineering* 53 (5) (2006) 959–963.
- [10] N. Haddad, R. B. Govindan, S. Vairavan, E. Siegel, J. Temple, H. Preissl, C. L. Lowery, H. Eswaran, Correlation between fetal brain activity patterns and behavioral states: an exploratory fetal magnetoencephalography study, *Experimental neurology* 228 (2) (2011) 200–205.
- 320 [11] D. F. Rose, H. Eswaran, Spontaneous neuronal activity in fetuses and newborns, *Experimental neurology* 190 (2004) 37–43.
- 325 [12] E. Fehlert, K. Willmann, L. Fritsche, K. Linder, H. Mat-Husin, F. Schleger, M. Weiss, I. Kiefer-Schmidt, S. Brucker, H.-U. Häring, H. Preissl, A. Fritsche, Gestational diabetes alters the fetal heart rate variability during an oral glucose tolerance test: a fetal magnetocardiography study, *BJOG: An International Journal of Obstetrics & Gynaecology* 124 (12) (2017) 1891–1898. doi:10.1111/1471-0528.14474.
- 330 [13] J. G. Nijhuis, H. F. Prechtl, C. B. Martin, R. S. Bots, Are there behavioural states in the human fetus?, *Early human development* 6 (2) (1982) 177–95.

- [14] J. Brändle, H. Preissl, R. Draganova, E. Ortiz, K. O. Kagan, H. Abele,
335 S. Y. Brucker, I. Kiefer-Schmidt, Heart rate variability parameters and fetal
movement complement fetal behavioral states detection via magnetography
to monitor neurovegetative development, *Frontiers in Human Neuroscience*
9 (2015) 147. doi:10.3389/fnhum.2015.00147.
- [15] M. Gertsch, *Das EKG: auf einen Blick und im Detail*, Springer-Verlag,
340 2008.
- [16] J. D. Wilson, R. B. Govindan, J. O. Hatton, C. L. Lowery, H. Preissl, Inte-
grated approach for fetal QRS detection, *IEEE Transactions on Biomedical*
Engineering 55 (9) (2008) 2190–2197. doi:10.1109/TBME.2008.923916.